Optics Communications 311 (2013) 90–99

Contents lists available at ScienceDirect

Optics Communications

journal homepage: www.elsevier.com/locate/optcom

Modeling and optimization of tapered-diode pumped Cr:LiCAF regenerative amplifiers

Umit Demirbas *

Laser Technology Laboratory, Department of Electrical and Electronics Engineering, Antalya International University, 07190 Dosemealti, Antalya, Turkey

ARTICLE INFO

Article history:
Received 1 June 2013
Received in revised form
16 August 2013
Accepted 18 August 2013
Available online 29 August 2013

Keywords:
Ultrafast laser amplifiers
Broadband solid-state laser gain media
Cr:LiCAF
Diode-pumping
Auger upconversion

ABSTRACT

We present a numerical study, which investigates the potential of diode pumped Cr:LiCAF regenerative amplifiers in detail. Special attention has been given to relevant material properties of the gain media, like the Auger energy transfer upconversion (ETU) process, to utilize the full potential of the material and to develop guidelines in choosing optimal material properties like chromium doping concentration and length. Moreover, importance of pulsed pumping, rather than continuous-wave (cw) pumping, in obtaining higher small signal gain values is discussed in detail. Effects of pump power, cavity losses, excited-state absorption, seed pulse energy, optical damage and ETU on obtainable pulse energies will also be presented. The modeling results have shown that, Cr:LiCAF regenerative amplifiers pumped by two 675 nm state-of-the-art 1-W tapered diodes have the potential to produce 50-fs long pulses around 800 nm with 70 μJ pulse energy and 1.4 GW peak power at repetition rates up to 5 kHz. Moreover, a 20-W diode pumped Cr:LiCAF amplifier has the potential to produce pulse energies of 1.1 mJ and peak powers of 20 GW. Expected optical-to-optical conversion efficiencies of the systems are about 30%. These results demonstrate that, with ongoing progress in laser diode technology, low-cost and efficient Cr:Colquiriite amplifiers has the potential to replace the expensive Ti:Sapphire technology in the future.

1. Introduction

Ultrashort optical pulses with high pulse energies and peak powers are useful for many applications including femtosecond micromachining [1], pump-probe spectroscopy [2], nonlinear optics [3], optical parametric amplifier pumping [4–6], and high harmonic generation [7]. The workhorse of femtosecond optics employing Ti:Sapphire technology, is the dominant source of use for such applications [8]. Today's commercial high-energy Ti:Sapphire systems can provide (i) ~3 μJ sub-40-fs pulses at up to 250 kHz (ii) >2.5-mJ energies with sub-25-fs pulses at up to 5 kHz, (iii) >100-mJ energies with sub-40-fs pulses at 10 Hz. Unfortunately, commercial Ti:Sapphire systems still use bulky, inefficient and high-cost pump sources in the green region of the spectrum that are based on second harmonic of Nd and Yb based laser systems. This non-optimum pumping limits widespread adoption of Ti:Sapphire based laser and amplifier technologies. Even though direct diode pumping of Ti:Sapphire gain medium with blue GaN diode lasers around 450 nm has been demonstrated recently, the obtainable average powers are only about 100 mW in femtosecond regime [9–12]. As an alternative, Neodymium, Ytterbium, Erbium, and Thulium doped solid state and fiber gain media facilitate efficient direct diode pumping, and have long upper state lifetimes, which enable better energy storage. However, due to their narrow gain bandwidths, the obtainable pulsewidths from these amplifiers are limited to several hundreds of femtoseconds [13–16]. Moreover, inherent high nonlinearity of fiber based amplifier systems limit the achievable pulse energies to 10 mJ level (so fiber amplifiers are more suitable for high average power, high repetition rate applications) [17–19].

Cr:Colquiriite oscillators/amplifiers (e.g. Cr:LiSAF [20], Cr:LiCAF [21], Cr:LiSGaF [22], Cr:LiSCAF [23] and LiChrom [24]), (i) enable efficient direct diode pumping with very low cost diodes around 650 nm, (ii) provide record high electrical-to-optical conversion efficiencies around 10%, (iii) have broad emission bandwidths around 800 nm to enable tunability from 720 nm to 1065 nm [21,25,26] and generation of sub-10-fs pulses [27–30], (iv) can be made quite compact, (v) have relatively long upper state lifetimes enabling energy storage, and (vi) have lower n_2 values that reduce unwanted nonlinear processes such as self-focusing and allows higher energy extraction per unit volume [31]. All of these properties make Cr:Colquiriite oscillators/amplifiers the leading efficient and low-cost laser/amplifier alternative to current Ti:Sapphire femtosecond technology.

Among colquiriites, Cr:LiCAF is the most suitable candidate for high power laser and amplifier applications due to its longer upper state lifetime, higher intrinsic slope efficiency [32], higher thermal

* Tel.: +90 553 239 0300.
E-mail address: umit79@alum.mit.edu

0030-4018/$ - see front matter © 2013 Elsevier B.V. All rights reserved.
http://dx.doi.org/10.1016/j.optcom.2013.08.059

conductivity [32], higher thermal quenching temperature [33], lower thermal lensing [34], lower quantum defect, lower excited-state absorption [20,21], and a lower upconversion rate [35]. However, to our knowledge, so far the highest pulse energy obtained from a diode pumped Cr:Colquiriite amplifier is only 10.5 μJ (pulse energy before compression, pulses are then compressed down to 170-fs level) [36,37]. We believe that, the relatively low performance of these initial studies is due to the low-brightness of pump diodes and high passive losses of the cavity optics that were available at that time. Moreover, in these initial studies the gain medium was pumped with continuous-wave diodes, which prevents acquiring higher single pass gain values due to thermal effects.

A variety of diodes have been exploited as pump sources for Cr:Colquiriite lasers and amplifiers, including single transverse-mode laser diodes [38], broad-stripe single-emitter diodes [39,40], and laser diode arrays [32]. One main drawback of these sources has been their relatively low brightness, which pushed researchers to combine four to six of these diodes to reach desired output power levels [26,40,41]. As an example, state-of-the-art single mode diodes around 650 nm provide about 170 mW of output power and have a brightness (B) of only about 360 mW/μm^2 ($M^2<1.1$). Single-emitter diodes with 150 μm stripe width provide up to 1.5 W output power, but their brightness is also low ($\sim$340 mW/μm^2), due to low quality output beam profile ($M^2_{slow}\sim 10$, $M^2_{fast}<1.1$). As an alternative diode technology, tapered diodes combine the good beam quality of ridge waveguide lasers and the high output powers of broad-stripe single emitter diodes in the same device [42,43]. For example, a single tapered diode on a C-mount package [43] could provide up to 1.2 W of output power at 675 nm together with M^2 ($1/e^2$) values of 1.1 in the fast axis and 2.6 in the slow axis. This corresponds to a brightness of about 1000 mW/μm^2, which is about three times improvement in brightness compared to the others. Hence, usage of tapered diodes enables dramatic simplification of pumping geometry, improves compactness and lowers cost in Cr:Colquiriite lasers and amplifiers [44].

In this work, we have investigated the performance of tapered diode pumped Cr:LiCAF regenerative amplifiers using detailed numerical analysis. Cr:LiCAF has been chosen among Cr:Colquiriites due to its better thermal characteristics, which is important for high power applications. In our amplifier model, effects such as excited-state absorption and Auger upconversion have been considered, to find the optimum crystal length, chromium doping concentration and pump focusing to achieve maximal gain and output pulse energy from the amplifier. The modeling results have pointed out that, Cr:LiCAF regenerative amplifiers pumped by two 1-W tapered diodes have the potential to reach pulse energies of 90 μJ ($\sim$70 μJ, $\sim$50-fs pulses with corresponding peak powers of $\sim$1.4 GW, at up to $\sim$5 kHz after compression). Furthermore, we have shown that, with expected future progress in diode technology, a hypothetical Cr:LiCAF amplifier that is pumped by a 20-W diode, has the potential to produce pulse energies of 1.1 mJ and peak powers of 20 GW. These results show that, with the recent tapered diode technology, 10-fold improvement in pulse energy and about 30-fold improvement in peak powers should be possible from directly-diode pumped, low-cost Cr:Colquiriite amplifiers [36,37,45–60]. These numbers will most probably scale further with ongoing progress in red laser diode technology. We hope that the presented results in this work will be helpful for laser engineers in designing optimal Cr:Colquiriite amplifiers.

The paper is organized as follows: Section 2 introduces the material properties of Cr:Colquiriite gain media that are relevant to amplifier design. Section 3 describes the numerical modeling used to simulate the amplifier performance. Section 4 presents the simulation results in detail. Finally, in Section 5, we summarize the results and provide a general discussion.

2. Material properties

As mentioned above, currently Ti:Sapphire lasers/amplifiers are the commercial standards for most of the femtosecond optics applications. However, their high cost presents a major obstacle and limits their widespread usability, slowing down progress in many important areas of science and technology. Lowering the cost of femtosecond technology can have a big impact on society, by accelerating research in basic and applied sciences. Among all the lasing materials, Cr^{3+}-doped Colquiriite crystals are the most promising low-cost alternative to Ti:Sapphire technology due to (i) their broad absorption bands around $\sim$650 nm which enables efficient direct diode pumping with low-cost diode lasers, and (ii) their broad emission bands around 800 nm enabling 10-fs pulse generation. In this section, we will review/compare material properties of Ti:Sapphire and Cr:Colquiriite gain media that are relevant for amplifier applications.

Compared to Ti:Sapphire, the emission cross section of Cr:Colquiriites is $\sim$8–32 times lower (Table 1). A lower emission cross section increases the tendency of the laser towards q-switched mode-locking instabilities, which might also manifest itself in amplifier applications. However, room temperature upper state lifetime of Cr:Colquiriites is $\sim$21–55 times longer than Ti:Sapphire. Hence, actually for Cr:Colquiriites the product of room

Table 1
Comparison of the spectroscopic and laser parameters of the Ti:Sapphire, Cr:LiSAF, Cr:LiSGaF, and Cr:LiCAF gain media.

Gain medium	Ti^{3+}:Al_2O_3 (Ti:Sapphire)	Cr^{+3}:$LiSrAlF_6$ (Cr:LiSAF)	Cr^{+3}: $LiSrGaF_6$ (Cr:LiSGaF)	Cr^{+3}:$LiCaAlF_6$ (Cr:LiCAF)
Gain peak [nm]	790	850	840	780
Tuning range [nm]	660–1180 [62]	780–1110 [63]	777–977 [26,64]	720–887 [21,65]
Demonstrated shortest pulse length [fs]	$\sim$5 [66]	10 [28]	14 [27]	9 [29]
Crystal figure of merit (FOM)	200	2000	2000	2000
Nonlinear refractive index (n_2) [10^{-16} cm^2/W]	3.2 [61]	0.8 [61]	1.2 [61]	0.4 [61]
Peak emission cross section (σ_{em}) [10^{-20} cm^2]	41 [67]	4.8 [67]	3.3 [22]	1.3 [67]
Room-temperature fluorescence lifetime (τ) [μs]	3.2 [67]	67 [67]	88 [22]	175 [67]
$\sigma_{em}\tau$ (μs) [10^{-20} cm^2]	131 [67]	322 [67]	290 [67]	228 [67]
Intrinsic slope efficiency [%]	64 [68]	53–54 [20,26]	52–60 [22,26]	67–69 [21,26]
Relative strength of excited-state absorption	0 [69]	0.33 [35]	0.33 [22]	0.18 [35]
Fracture toughness [MPa m$^{1/2}$]	2.2 [70]	0.4 [70]	–	0.31 [70]
Thermal conductivity [W/K m]	28 [70]	3.1 [70]	3.6 [61]	5.1 [70]
$T_{1/2}$, $\tau_f(T_{1/2})=0.5\tau_R$ [C]	$\sim$100 [69]	69 [33]	88 [34]	255 [33]
Thermal expansion coefficient [10^{-6}/K]	5.3 [70]	25 [22]	–	22 [22]
Thermal shock resistance [W/m$^{1/2}$]	22 [70]	0.4 [70]	–	0.5 [70]
Auger upconversion rate (γ) [10^{-16} cm^3/s]	–	6.5 [35]	6.5 [35]	1.65 [35]

temperature upper state lifetime and emission cross section ($\sigma_{em}\tau$) is ~2–2.5 times higher, hence enabling lower-threshold laser operation during the cw pumping regime for the same resonator design. Another major advantage of Cr:Colquiriites is the ability to grow high quality crystals with minimal passive losses below 0.15% per centimeter [63,65,71]. Hence, the figure of merit (FOM) of Cr:Colquiriite crystals is about one order of magnitude higher than those for Ti:Sapphire (Table 1). Combined with the larger ($\sigma_{em}\tau$) product, this results in record low lasing thresholds (~2–3 mW) in Cr:Colquiriites. The quality of the gain media (the passive loss level) is also a quite important factor in amplifier performance, as we will discuss in more detail in Section 4. In general a higher $\sigma_{em}\tau$ product also means a higher small signal gain, since small signal gain is proportional to the product of emission cross section and population inversion. However, as we will try to describe in detail below, the upper state lifetime of Cr:Colquiriites can be effected severely by a number of different physical processes, and one should be careful in the amplifier design to utilize the full potential of Cr:Colquiriite gain media.

In chromium-doped colquiriites, there are four main mechanisms that contribute to thermal loading inside the crystal: (a) quantum defect, (b) thermal quenching of the upper laser level, (c) excited-state absorption, and (d) upconversion (Fig. 1). The first of these effects is quantum defect, which is due to the energy difference between the laser (ω_l) and pump (ω_p) photons. The difference in energy is transferred to the crystal via nonradiative transitions (phonon emission), and cause an inevitable thermal loading. The thermal load caused by the quantum defect is linearly proportional to the pump power and is in general, not the major heat source for Cr:Colquiriites since pump and laser/seed wavelengths are very close to each other (~650 nm and ~800–850 nm). Moreover, for Cr:Colquiriites, the quantum defect is lower compared to Ti:Sapphire, since Ti:Sapphire lasers have lower pump wavelengths (~532 nm versus ~650 nm). Note that, among the Cr:Colquiriites, Cr:LiCAF has the lowest quantum defect due to its blue shifted emission spectrum.

The second effect, thermal quenching of the upper laser level $|l\rangle$, causes thermal loading and depopulation of the upper state laser level ($|l\rangle$) at the same time. The upper state lifetimes of the Cr^{3+}-doped colquiriites are temperature-dependent and for temperatures above a critical value ($T_{1/2}$ in Table 1), thermal quenching starts to cause significant nonradiative decay of the excited-state ions from the upper laser level $|l\rangle$ to the ground state $|g\rangle$ (here the critical temperature, $T_{1/2}$ [33], is the temperature at which the fluorescence lifetime drops to half of the radiative lifetime value). For transition metal ion-doped laser materials, the Mott equation is generally used to describe the strength of temperature-dependent nonradiative relaxation processes [72,73]. In this model, the temperature dependence of the fluorescence lifetime $\tau_F(T)$ is given by

$$\frac{1}{\tau_F(T)}=\frac{1}{\tau_R}+\frac{1}{\tau_{NR}(T)}=\frac{1}{\tau_R}+\frac{1}{\tau_{NR0}}\mathrm{Exp}\left(-\frac{\Delta E}{kT}\right) \quad (1)$$

Here, τ_R^{-1} is the spontaneous radiative decay rate, $\tau_{NR}(T)^{-1}$ is the temperature-dependent nonradiative decay rate, $\tau_{NR0}{}^{-1}$ is the high temperature limit of the nonradiative decay rate, ΔE is the activation energy, k is Boltzmann's constant and T is the absolute temperature in degrees Kelvin. Fig. 2 shows the calculated variation of fluoresce lifetime with temperature for Cr:Colquiriites using Eq. (1) and the parameters that are used in the calculation is from Table 1 [33,34].

Among all the four heating mechanisms, the thermal quenching process, which decreases the gain of the crystal, is the most destructive one. This is because of the cascading nature of this mechanism; the rate of heat generation via thermal quenching is itself temperature-dependent. Once thermal quenching becomes significant, additional heating increases its rate even further in an exponential manner. This finally leads to a rapid decay of all the excited ions to the ground state via thermal quenching, and all of the absorbed pump power is converted into heat. This can even cause permanent damage to the crystal. Therefore, for efficient laser/amplifier operation, the crystal temperature should be always well below $T_{1/2}$. For Cr^{3+}:LiCAF the critical temperature for thermal quenching is quite high ($T_{1/2}$=255 °C) [33], and for internal crystal temperatures below ~150 °C, thermal quenching is not a significant heating mechanism (Fig. 2). The main drawback of Cr^{3+}:LiSAF and Cr^{3+}:LiSGaF is their low critical temperature ($T_{1/2}$=69 °C for Cr^{3+}:LiSAF and 88 for Cr^{3+}:LiSGaF) [33,34], which sets a barrier in laser/amplifier output power scaling [32,40,74,75]. It is mainly the higher critical temperature of Cr^{3+}:LiCAF that enables power scaling in laser/amplifier applications.

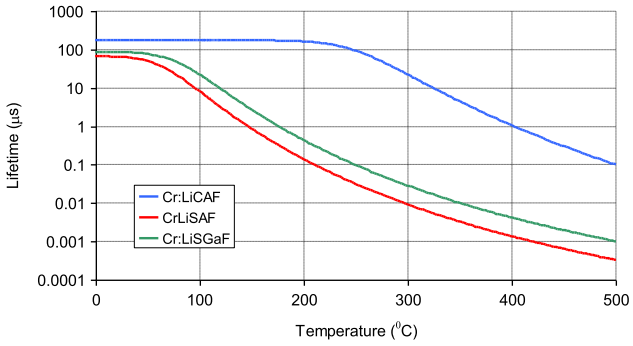

Fig. 2. Calculated effect of temperature (thermal quenching) on fluorescence lifetimes of Cr:LiCAF, Cr:LiSAF and Cr:LiSGaF gain media.

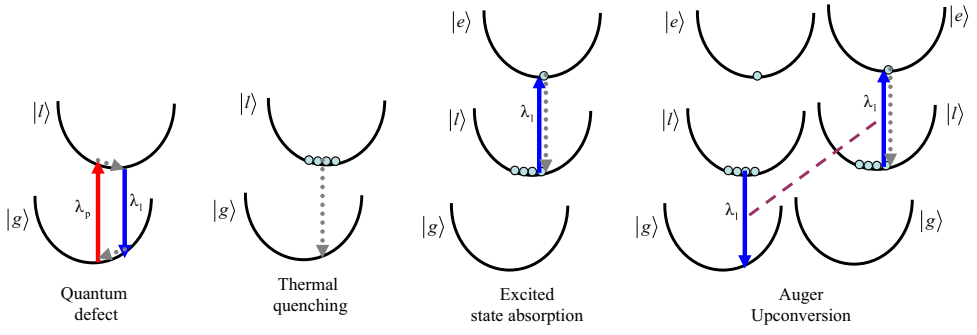

Fig. 1. Quantum defect, thermal quenching, excited-state absorption and the Auger upconversion effects that cause thermal loading in Cr^{3+}-doped colquiriites. See the text for a detailed explanation of each process.

The third mechanism that causes thermal loading is excited state absorption (ESA), where an ion in the upper laser level $|l\rangle$ absorbs a laser or a pump photon and gets promoted to a higher lying excited level $|e\rangle$. The ion then relaxes back to the upper laser level $|l\rangle$ via nonradiative decay, and hence heats up the crystal. For Cr^{3+}:Colquirrites, ESA at pump wavelengths is quite low, but there is significant ESA at the lasing wavelengths (becomes more prevailing at longer wavelengths above ~850 nm) [20–22,31,76–79]. Relative strength of ESA (σ_{ESA}/σ_{em}) in Cr:LiCAF (~0.18) is lower compared to Cr:LiSAF/LiSGaF (~0.33), which is a significant advantage for an amplifier gain medium. We will describe the effect of ESA on the obtainable output pulse energies from the amplifier in the next section.

The last mechanism that creates thermal loading in Cr^{3+}: Colquirrites is the Auger energy transfer upconversion (ETU) process [80], which is similar to the ESA. However unlike ESA, the upconversion process does not require the presence of external photons to occur. In this process, ions at the upper laser level $|l\rangle$ interact with each other, where one of the ions decays to the ground state $|g\rangle$ and the created energy from this decay transfers another neighboring ion to the upper lying excited level $|e\rangle$. Again, the ion in the excited state $|e\rangle$ non-radiatively decays back to the laser level $|l\rangle$ and heats up the crystal. Caused by the interaction of the ions in the upper laser level, the upconversion process scales with the square of the upper state population density, and hence could generate a significant heat load at high pumping intensities. Due to the ETU process, the fluorescence lifetime becomes dependent on inversion density, and this dependence can be estimated using

$$\frac{1}{\tau_F(N)} = \frac{1}{\tau_R} + \gamma N \tag{2}$$

where N is the population inversion density of the laser level $|l\rangle$ and γ is the Auger energy transfer upconversion rate. Fig. 3 shows the calculated variation of fluoresce lifetime with population inversion density for Cr:Colquiriites using the Auger upconversion rates given in Table 1 [35]. Since Auger upconversion process rate does not depend on temperature, it is quite effective even at low temperatures. Due to ETU, the upper state lifetime of Cr:LiCAF decreases to half of its value at a population inversion density of 3.6×10^{19} ions/cm^3. For Cr:LiSAF/Cr:LiSGaF Auger upconversion rate is even higher, and the critical inversion density is only around 2.3×10^{19} ions/cm^3. Auger upconversion significantly limits the population inversion densities (and hence the small signal gain values) one can obtain in Cr:Colquiriites; hence, it is a very important factor to consider for an efficient laser or amplifier design. Again, we will describe the effect of ETU on the obtainable output pulse energies in the following sections.

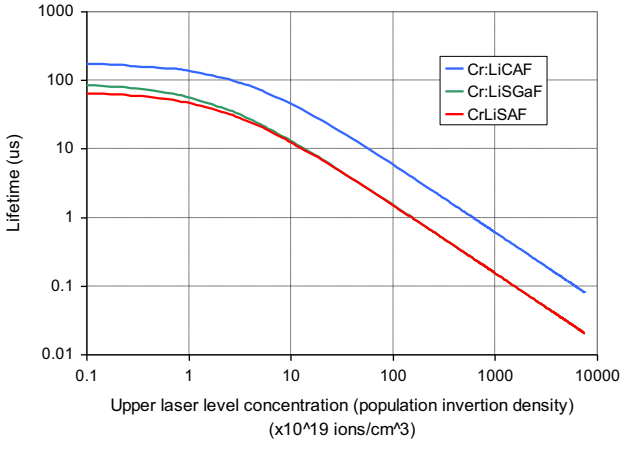

Fig. 3. Calculated effect of Auger upconversion process on fluorescence lifetimes of Cr:LiCAF, Cr:LiSAF and Cr:LiSGaF gain media.

3. Numerical modeling of amplification

Fig. 4 shows a schematic of the Cr:LiCAF regenerative amplifier that was used in the modeling. The assumed setup is quite standard for regenerative amplifier applications, and is similar to what was employed in the previous experimental studies [36,37]. A Brewster cut Cr:LiCAF gain medium with doping D, and length L was supposed to be used as the gain medium. We have assumed here that the Cr:LiCAF crystal absorbs almost all the incident pump light (> 99%). For example this corresponds to a Cr-doping level of 10% for a 2 mm crystal, 5% for a 4 mm crystal and 2% for a 10 mm crystal. As will be described in detail below, all the possible options are considered in the analysis to find the optimum crystal length and concentration for such a study. The cavity is x-shaped and consists of two curved and two flat high reflectors. A thin film polarizer and a Pockels cell pair are used to couple in (out) the input (output) pulse. Distributing the population inversion within the crystal homogeneously is quite important for obtaining the highest possible small signal gain from the amplifier at a fixed pump rate. Hence, two TM-polarized 1-W tapered diodes will pump the amplifier from each side, to obtain a homogenous distribution of inversion within the crystal. Previous experimental studies with the tapered diodes have shown that good mode matching between the tapered diode pump and laser/amplifier cavity modes could be obtained [44]. Here we have assumed that, due the imperfect beam profile of the tapered diode, the mode matching between the pump laser mode and the amplified pulse mode is limited to 90%. While pumping the regenerative amplifier, the diodes will be operated in pulsed mode with pulsewidths of 10s of microseconds (total peak power will stay same at ~1W from each diode). For example, at 1 kHz repetition rate, with a ~100 μs pulsewidth, this corresponds to a duty cycle of only 10%, and an average power of only 100 mW from each diode. We have shown that, compared to cw pumping, pulsed pumping (quasi-cw-pumping) reduces the thermal effects and enables tighter focusing inside the crystal. Tighter focusing facilitates lower saturation fluencies and higher small signal gain, which increases extraction efficiencies and reduces the number of round trips required in the regenerative amplifier. In our numerical analysis, for each Cr:LiCAF crystal length and concentration, we have determined the optimum beam waist and the optimum pump pulse duration, which will be discussed in more detail below.

In the simulations, the cavity is assumed to have a total loss of 2%. Actually, recent studies have shown that, due to the latest improvements in crystal growth and mirror coating technology, high figure of merit Cr:LiCAF crystals and high quality mirrors are commercially available. A Cr:LiCAF laser cavity with round-trip passive losses below 0.2% and a crystal FOM above 2000 has been reported recently [65]. The remaining 1.8% loss is assumed to be present in the thin film polarizer and the Pockells cell, which is a quite safe estimate for today's high quality devices.

The input seed pulses to the amplifier will be provided by a low-cost Cr:LiCAF laser, and the optical spectrum will be centered around 800 nm with a FWHM of around 20–25 nm (corresponds to about 25–30 fs transform limited pulses). The input pulse energy is assumed to be 1 nJ in the analysis. To keep the self phase

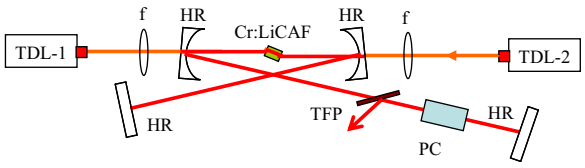

Fig. 4. Schematic of the Cr:LiCAF regenerative amplifier pumped by two 1 W tapered diodes. f: Focusing lens, HR: high-reflecting mirror, TFP: thin film polarizer, PC: pockels cell.

modulation effects low and also to prevent damage to the cavity optics/coatings the pulses for the amplifier are assumed to be stretched to ~200 ps level (B-integral around 1). We note here that, due to their lower nonlinear refractive index values (n_2), required stretching for Cr:Colquiriite based amplifiers is lower compared to Ti:Sapphire (Table 1). For example, stretching a ~30-fs pulse to ~100-ps requires a second order dispersion of ~10^6 fs^2. We presumed that dielectric diffraction grating pairs with an estimated throughput of 80% will be used in the compressor. Moreover, we have assumed that for pulse fluencies above 5 J/cm^2 [81] material damage will occur in Cr:LiCAF gain media.

We have used Frantz–Nodvik equation for the numerical modeling of the amplification process. Accroding to Frantz–Nodvik model, if the duration of the amplified pulse and the time of flight through the amplifying medium is short compared to the fluorescence lifetime of the gain medium, then one can neglect spontaneous emission and use the following analytical equation for the amplification process in an amplifier [37,82]:

$$J_{out} = J_{Sat} Ln[1 + e^{\eta g_0}(e^{J_{in}/J_{sat}} - 1)] \quad (3)$$

Above $J_{in}(J_{out})$ is the incident (output) pulse fluence, J_{Sat} is the saturation fluence of the gain medium ($J_{Sat} = h\nu/\sigma_{em}$), J_{Sto} is the stored energy density ($J_{Sto} = (E_{abs}/A_{eff})(\lambda_P/\lambda_L)$), E_{abs} is the stored pump energy, A_{eff} is the effective pump beam area, g_0 is the small signal gain (($g_0 = J_{sto}/J_{sat} = (E_{abs}/(h\nu_L))(\sigma_{em}/A_{eff})$), and η is a factor that considers the effect of ESA on the amplification ($\eta = 1 - \sigma_{ESA}/\sigma_{em}$). In order to solve for the evaluation of the pulse energy in the amplifier, we have applied Eq. (3) iteratively, with the output energy of the nth pass taken as the input energy of the $(n+1)$th pass. In each pass, the variation in the stored energy in the upper laser level and the effect of cavity losses are also included. While determining g_0, we have considered limitations due to ETU and others as will be described in more detail in the next section.

Similarly, the effect of gain narrowing in the amplifier can be modeled using [37,83]:

$$\Delta\lambda = \Delta\lambda_0 / \sqrt{1 + Ln(G)(\Delta\lambda_0/\Delta\lambda_{Fluo})^2} \quad (4)$$

where $\Delta\lambda_0$, $\Delta\lambda$ and $\Delta\lambda_{Fluo}$ represent the spectral width of the seed pulse, amplified pulse and the gain widths of the amplifying medium, respectively, whereas G is the overall accumulated gain of the amplifier. For example, for a Cr:LiCAF regenerative amplifier that amplifies a 1-nJ 30-fs pulse to 1 mJ (G=100,000), gain narrowing will limit the minimum obtainable pulsewidths to ~45 fs level. A similar total gain will increase the pulsewidth of a 10-fs pulse to around 35-fs; hence, using a very broad seed source only incrementally helps with the expected pulse durations. As a safe value, in our analysis, we have assumed that the output pulses will be compressible down to 50 fs.

4. Simulation results

In this section, we will present the simulation results for the tapered diode pumped Cr:LiCAF regenerative amplifiers in detail. To start with, Fig. 5 shows the calculated variation of output pulse energy for Cr:LiCAF crystals with different lengths at a total incident TDL pump power of 2 W. In our analysis, to make a fair comparison between different crystals, we have assumed that the chromium doping levels have been adjusted, so that all the crystals have the same percentage of pump power absorption (around 99%). Pulsed pumping is applied to the regenerative amplifier. The repetition rate of the pulses is assumed to be 1 kHz and the pump pulse duration is optimized for each case to obtain the maximum pulse energy. As we mentioned above, pumping continuously at a fixed average power of 2 W is not optimum due

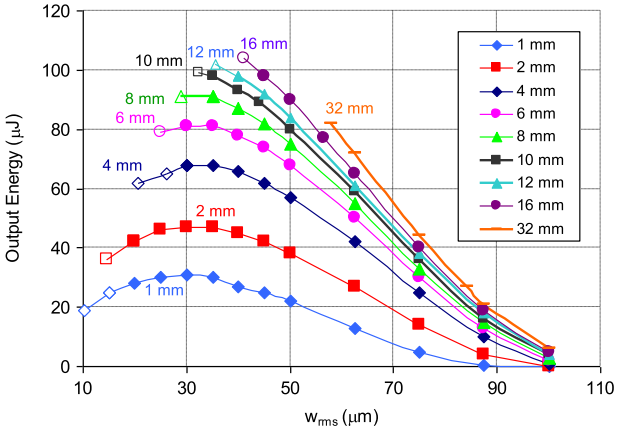

Fig. 5. Calculated variation of output pulse energy with the rms (root mean square) value of pump spot size inside the Cr:LiCAF medium at a total TDL pump power of 2 W. The calculation has been performed for Cr:LiCAF crystals with different lengths (1–32 mm). All the crystals are assumed to have a pump absorption of around 99% (the doping level decreases with increasing length). Markers with an empty background represent energy fluence values that can possibly cause material damage to the Cr:LiCAF media.

to the presence thermal effects. Also pumping with a pump pulse duration of 175 μs (fluorescence lifetime of Cr:LiCAF) is not optimum, since for most of the cases, due to Auger upconversion and thermal quenching, the lifetime of the crystal decreases to a much lower value. Hence, in the optimization process, our simulations have first searched for the optimum pulsed pumping condition for the amplifier, and then performed the Frantz–Nodvik analysis. The case of pulsed pumping will be described in more detail below.

Fig. 5 also shows the calculated variation of pulse energy with pump focusing. Here, we have used the rms (root mean square) value of pump spot size (w_{rms}) inside the Cr:LiCAF crystal, rather than pump beam waist (w_0), to account for the variation of beam waist within the focus depth. As an example, for the 1 mm long Cr:LiCAF crystal, due to the short crystal length, it is possible to obtain very tight focusing with short Rayleigh ranges (w_{rms} as low as 10.25 μm, and w_0 as low as 7.25 μm). This is expected to produce the highest population inversion density, which in turn should produce the highest gain and the highest output pulse energy for an ideal medium (note that a tighter focus decreases saturation energy and increases extraction efficiency). However, in the case of Cr:LiCAF due to the presence of Auger upconversion (dependence of lifetime on population inversion), the optimum focusing for the pump is actually around 30 μm. If one focuses tighter than that, the population inversion density gets too high, and then ETU decreases the fluorescence lifetime significantly (Fig. 6). Actually, for 10 μm focusing, the optimum pump pulsewidth is only around 20 μs (Fig. 6), and with that the gain medium can only store 31 μJ of energy. Due to tight focusing, the single pass gain is as high as 35%, and the amplifier can extract 63% of this energy to produce an output pulse energy of 19 μJ. Hence, even though the extraction efficiency is high, due to the low amount of stored energy, the overall output is low for tight focusing. On the other hand, the optimum pump pulsewidth increases to 50 μs level for an rms spot size of 30 μm. Then with increased pumping duration, the crystal can store more energy (80 μJ). However, the single pass gain (11%) and the extraction efficiency (38%) are lower due to the increased spot size, and the output pulse energy increases to 30 μJ level. We note here that, by increasing the spot size even further above 30 μm, one can decrease the role of ETU, and increase the stored energy via increased pump pulse duration. However, for very weak focusing, the single pass gain decreases too much, and the saturation energy increases by a large amount, which considerably decreases the extraction efficiencies and hence the output pulse

energies (see the curve for 1 mm crystal in Fig. 5). Lastly, we should note that when focusing very tight, the circulating intracavity pulse energy can actually exceed the damage threshold of the material (5 J/cm^2 [81]). In Fig. 5, these points are shown with markers with an empty background, and possibly could not be achieved due to material damage.

As we see from Fig. 5, at the total incident peak pump power of 2 W, the optimum Cr:LiCAF crystal has a length of about 10 mm and a Cr-doping level of 2% (crystals with a length of 8, 12 and 16 mm also give similar results). Table 2 lists the variation of amplifier parameters with pump beam size for the 10 mm crystal. The highest output energy (98 μJ) is obtained for a beam waist of about 35 μm (rms value). For tighter focusing, the intracavity circulating pulse energy fluence exceeds the damage threshold of Cr:LiCAF gain media. The optimum pump pulsewidth is calculated as 124 μs, which is quite close to the Cr:LiCAF fluorescence lifetime. With that, once can store up to 189 μJ of pulse energy within the gain medium, and could reach small-signal gain values around 18.3%. The required number of round trips is around 110, which takes around 1 μs in a standard 100 MHz cavity. Moreover, the overall B-integral is estimated to be around 0.71, which shows that initial chirp (200 ps) is enough to keep the nonlinear effects at a reasonably low level. However, we note here that, in the calculation of B-integral, we have ignored contributions from the Pockels cell and thin-film polarize. Nonlinear contributions from these elements are not always negligible in reality, and pulses with larger chirp might be required in the experiments. Assuming a total throughput efficiency of about 80% in compression, the output pulses will have around 78 μJ pulse energy, 50-fs pulsewidth, around 1.4 GW of peak power (assuming sech^2 pulse shape). The total process (pumping and amplifying action) is expected to take around 125 μs, so we expect that, the repetition rates can be increased to 8 kHz level without sacrificing too much from the above mentioned specs. At a repetition rate of 8 kHz, the expected average powers are around 545 mW, corresponding to an optical-to-optical conversion efficiency above 28%.

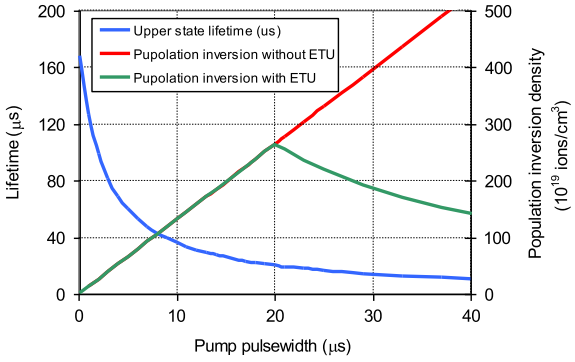

Fig. 6. Calculated variation of fluorescence lifetime and population inversion with input pump pulsewidth, for a 1 mm long, 20% Cr-doped Cr:LiCAF crystal at an incident peak power of 2 W (as shown in Fig. 4, the crystal is assumed to be pumped by two 1-W diodes, one from each side). The optimum pump pulse duration for this case is around 20 μs. Using longer pump pulsewidths will actually decrease the inversion and the stored energy.

We have seen from the results above that, for a total pump power of 2 W, the optimum crystal for the regenerative amplifier is a 2% Cr-doped, 10 mm long Cr:LiCAF. However, by pumping the amplifier with more diodes, or in the future with the availability of higher power diodes, the total incident pump power on the system can be increased. For this purpose, we have also investigated the Cr:LiCAF regenerative amplifier performance for incident peak pump power levels ranging from 1 W to 20 W. Fig. 7, which shows the variation of obtainable pulse energies for different crystal lengths at different pump power levels summarizes the simulation results for this case. Note that, due to the presence of ETU, as the available pump power increases, the optimum Cr:LiCAF crystal length for regenerative amplification applications increases. Also for the 5 W and 20 W cases, markers with an empty background similarly shows results with an intracavity circulating pulse energy fluence above the damage threshold of the Cr:LiCAF material. Hence, for these cases, the spot size inside the Cr:LiCAF amplifier is increased to decrease the fluence to a safe level. The side effect is a decrease of around 10% in obtainable pulse energies (markers with filled-in background).

As an example, at a total pump power of 20 W, we expect the amplifier to produce pulse energies as high as 1365 μJ using a 0.4% Cr-doped 50 mm long Cr:LiCAF crystal. For this case, the optimum rms value of pump beam is 110 μm, the optimum pump pulsewidth is 158 μs, the small signal gain is around 23.6%, the stored energy is 2400 μJ, the required round trips is around 100, the corresponding extraction efficiency is 57%, and the overall B-integral is around 3.5 (one can increase the chirp of the input pulses to around 500 ps level to decrease the B integral value 1.5). Assuming a total throughput efficiency of about 80% in pulse compression, the output pulses will have around 1.1 mJ pulse energy, ~50-fs pulsewidth, and around 20 GW peak power. The expected average power is 6.6 W at a repetition rate of 6 kHz, which corresponds to an optical-to-optical conversion efficiency of 33%. To summarize, we have seen that, with increased pump power, optimum crystal length increases, optimum crystal doping decreases, optimum pump beam waist increases, the stored energy, gain and required number of round trip decreases and the output pulse energy and the B-integral increases. Hence, we have seen that pump power level has a significant importance in

Table 2
Simulation results of the single-mode diode pumped Cr:LiCAF regenerative amplifier pumped by two 1-W tapered diodes.

w_{rms}/w_0 (μm)	Optimum pump pulse-width (μs)	Single pass gain (%)	Stored energy in the gain medium (μJ)	Saturation energy of the gain medium (mJ)	Output pulse energy (μJ)	Required # of round trips	Extraction efficiency (%)	B-integral
32.5/23[a]	120	20.5	183	887	99	95	54	0.68
35/30.5	124	18.3	189	1029	98	110	52	0.71
40/37.5	131	14.8	200	1344	94	135	47	0.62
45/43.5	137	12.2	209	1700	89	170	43	0.53
50/49	143	10.3	216	2100	80	210	37	0.47
62.5/62	151	7	230	3282	59	350	26	0.36
75/74.5	157	5.1	239	4725	36	580	15	0.25
87.5/87.5	161	3.8	245	6468	16	1050	6.5	0.16
100/100	164	2.9	249	8401	4	2300	1.6	0.06

The results are for a 2% Cr-doped 10 mm long crystal, and shows the effect of pump focusing on several amplifier parameters including, optimum pump pulsewidth, single pass gain, stored energy, saturation energy, required number of round trips, extraction efficiency, output pulse energy and B-integral.

[a] For the spot size (w_0) of 23 μm, the intracavity circulating pulse energy fluence exceed the damage threshold of Cr:LiCAF material.

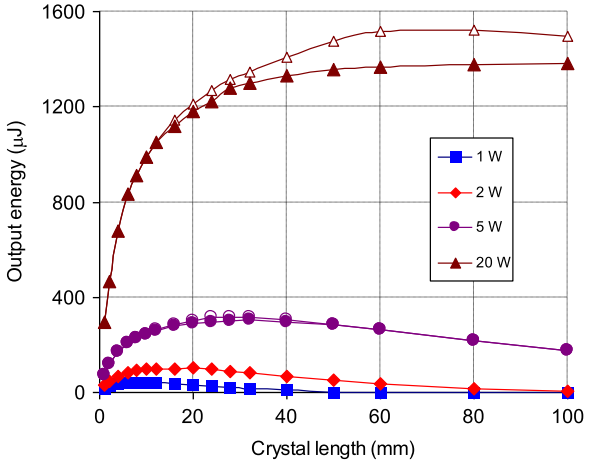

Fig. 7. Calculated variation of output pulse energy with crystal length at different total pump power levels. All the crystals are assumed to have a pump absorption of around 99% (the doping level decreases with increasing length).

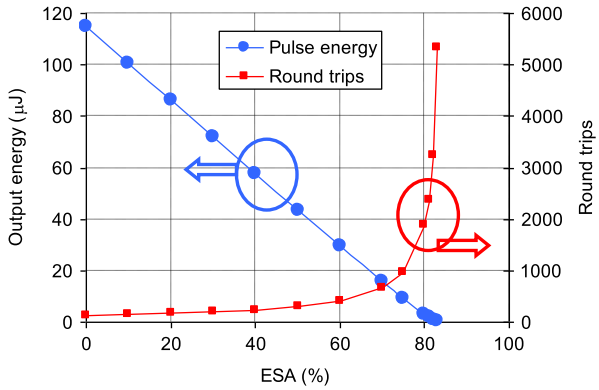

Fig. 8. Calculated variation of output pulse energy and required number of round trips for amplification, for the 2% Cr-doped 10 mm long Cr:LiCAF crystal as a function of excited state absorption. The peak pump power is taken as 2 W, and the rms value of pump beam size inside the crystal is taken as 45 μm.

determining the optimum parameters for the Cr:LiCAF regenerative amplifiers.

In the remaining part of this section, we will investigate how several parameters like ESA, ETU, cavity losses and input pulse energy effects the Cr:LiCAF regenerative amplifier characteristics (Figs. 8–11). For all the cases, we have assumed that, a 2% Cr-doped, 10 mm long Cr:LiCAF crystal is used as the gain medium, the total incident pump peak power is 2 W and the rms value of pump beam size inside the crystal is 45 μm (w_0 is around 43.5 μm). To start with, Fig. 8 shows the calculated variation of output pulse energy and required round trips as a function of relative strength of excited state absorption (ESA%:σ_{ESA}/σ_e). Fig. 8, clearly points out the detrimental effect of ESA on obtainable pulse energies: accessible pulse energy decreases linearly with ESA. With increasing ESA, the required number of round trips also increases due to the decrease in extraction efficiency. One advantage of Ti:Sapphire as an amplifier medium is, it does not suffer from ESA (Table 1). Among Cr:Colquiriites, Cr:LiCAF has the lowest relative strength of ESA (18% [35]), which gives it an advantage over other Colquiriites (33% [22,35]) in laser/amplifier applications. Fig. 8 also demonstrates that, keeping all the other parameters same, if Cr:LiCAF did not have any ESA; the obtainable pulse energies would increase from 89 μJ to 115 μJ (about 30% increase). Basically, 26 μJ of energy is converted into phonons via the ESA process.

Similarly, Fig. 9 displays the effect of the Auger energy transfer upconversion (ETU) process on the obtainable output pulse

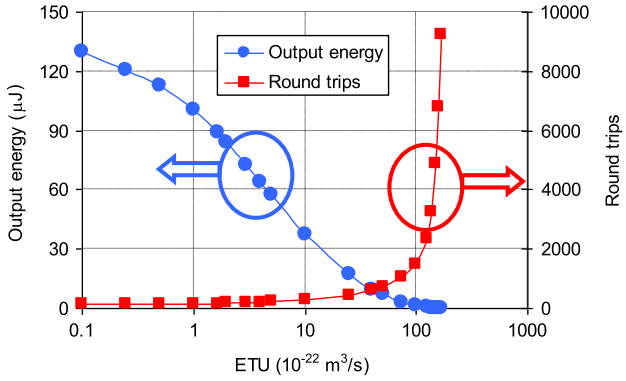

Fig. 9. Calculated variation of output pulse energy and required number of round trips for amplification, for the 2% Cr-doped 10 mm long Cr:LiCAF crystal as a function of ETU rate. The peak pump power is taken as 2 W, and the rms value of pump beam size inside the crystal is taken as 45 μm.

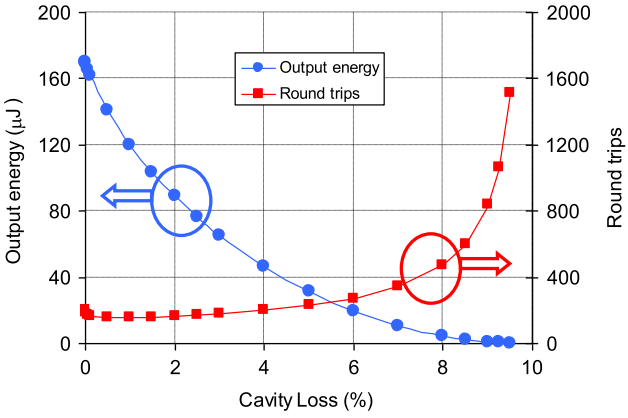

Fig. 10. Calculated variation of output pulse energy and required number of round trips for amplification, for the 2% Cr-doped 10 mm long Cr:LiCAF crystal as a function of round trip cavity losses. The peak pump power is taken as 2 W, and the rms value of pump beam size inside the crystal is taken as 45 μm.

energies and required number of round trips. Note that the presence of ETU limits the obtainable pulse energies in a very sharp manner, due to limitations it exposes on energy storage capacity of the gain medium (notice that the *x*-axis in Fig. 9 is in logarithmic scale, and the decrease of obtainable pulse energies with ETU is quite fast). Again, among Cr:Colquiriites, Cr:LiCAF has the lowest amount of ETU (1.65×10^{-22} m^3/s [35]), which gives it an important advantage in laser/amplifier applications. Assuming a zero level of ETU for Cr:LiCAF, the obtainable pulse energies would increase from 89 μJ to 130 μJ (around 40 μJ is lost due to ETU). Ti:Sapphire which does not suffer from ETU process, also have a clear advantage compared to Cr:Colquiriites in that manner. As we tried to describe in detail above, the presence of ETU process requires careful optimization of the gain medium length, gain medium chromium concentration, and pump focusing level to reach higher output energy levels from Cr:Colquiriite amplifiers.

Another important parameter that affects the regenerative amplifier performance is the round-trip passive losses of the amplifying cavity. Fig. 10 plots the calculated variation of output pulse energy as a function of round-trip cavity losses. As mentioned above, in our analysis, to be on a safe side, we have assumed a total round-trip loss level of 2% (around 0.2% from the Cr:LiCAF crystal and 1.8 from the pulse thin film polarizer and the Pockells cell). Simulation results have shown that, this 2% loss decreases the obtainable pulse energies from about 170 μJ to 89 μJ. ESA and ETU is not within the control of laser engineer, but the results show that, for a Cr:LiCAF amplifier with limited gain, it well worth to be careful in minimizing the passive losses of the cavity

by using the lowest loss TFP and Pockells cells in the market. As mentioned earlier, Ti:Sapphire crystals have a loss level of around 2% per cm and a FOM of about 150 for reasonably doped samples (which is around 10 times worse than Cr:LiCAF) [10]. Hence, the FOM advantage of Cr:Colquiriites enables the construction of high-Q-cavities [65], where one can store energy efficiently, and as we see, this is quite important for amplifier applications. Lastly, as we also mentioned earlier, we believe that the relatively low performance of initial diode-pumped Cr:LiCAF amplifier results is partly due to the high passive losses of the cavity optics (3.2%) that were available at that time [36,37].

Fig. 11 further shows the calculated variation of output pulse energy as a function of input/seed pulse energy. Note that the *x*-axis here is in logarithmic scale and for seed pulse energies from 1 fJ to 10 μJ the output energy is stable around 90 μJ. However, we note here that, for very low seed pulse energies, issues like gain narrowing, signal-to-noise ratio and amplified spontaneous emission background might become a problem, which is not included in our model. Also note that, as the seed pulse energies reach the saturation energy level, a single pass through the gain medium extracts almost all the stored energy. In our analysis, we have assumed a quite reasonable seed pulse energy level of 1 nJ, which is easily obtainable from standard low-cost Cr:Colquiriite lasers [26,65]. Analysis has also shown that, the effect of seed pulse energy is minimal on the performance of the amplifier, and it is not worth the increased cost and complexity to use higher energy Cr:Colquiriite systems [84,85].

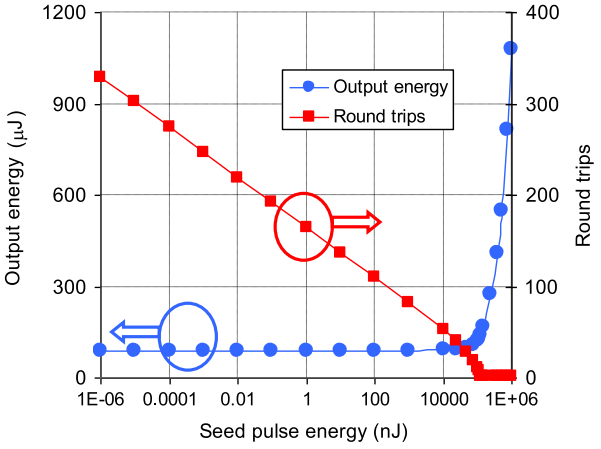

Fig. 11. Calculated variation of output pulse energy and required number of round trips for amplification, for the 2% Cr-doped 10 mm long Cr:LiCAF crystal as a function of seed pulse energy. The peak pump power is taken as 2 W, and the rms value of pump beam size inside the crystal is taken as 45 μm.

Lastly, we would like to compare our simulation results with, what is already achieved within the literature. For this purpose, Fig. 12 plots the obtained peak powers and pulse energies from Cr:Colquiriite amplifiers to date using several different pump sources including flashlamps, Argon/krypton ion lasers and diodes [36,37,45–60]. We have also included the simulation results of tapered diode pumped Cr:LiCAF amplifier in Fig. 12 (2-W pumped system). Moreover, simulation results with hypothetical 20-W pumped systems are also included to get an idea about possible improvements that awaits us in the future. Clearly, at very low repetition rates, flashlamp pumping enables the generation of highest peak powers. For example, Beaud et al. demonstrated 90-fs, 750 mJ pulses, from a 4-stage (1 regenerative and 3 multipass) amplifier pumped by flaslamps [48]. However, the repetition rate was only about 0.02 Hz (1.25 mW average power), and moreover the system is quite complex, very inefficient and high-cost. As an alternative, Argon/Krypton ion laser pumped Cr:Colquiriite amplifier systems work at higher repetition rates, but these systems do not posses any clear advantage when compared to Ti:Sapphire based technology. Moreover, the demonstrated performance of Cr:Colquiriite amplifiers pumped by Argon/Krypton ion lasers is also quite limited (210 fs pulses with 6.5 μJ pulse energy, 30 mW peak power at up to 5 kHz) [56,57]. Despite their potential, there is limited number of earlier work, with directly diode pumped Cr:Colquiriite amplifiers [36,37,57,59,60]. The highest pulse energy reported in these studies is 10.5 μJ (pulse energy before compression, pulses are then compressed down to 170-fs level) [36,37]. Our detailed analysis have shown that, by using optimum crystal doping/length, and by using pulsed pumping approach to minimize thermal effects (especially from ETU), today's tapered diode pumped Cr:LiCAF regenerative amplifiers have the potential to generate up to 98 μJ pulse energies using simple amplifier geometries (2-W pumped system), and up to 1.35 mJ from more complex systems that we expect to be available in the future (20-W pumped system) at up to 5 kHz repetition rate. We believe the optimization rules described in this work, have the potential to be quite useful for the laser engineers for optimal design of Cr:Colquiriite amplifiers.

5. Summary and discussion

In this work, we have investigated the potential of diode-pumped femtosecond Cr:LiCAF regenerative amplifiers as a low-cost, compact and efficient alternative to the existing Ti:Sapphire amplifier technology. The simulation results have shown that, a minimal complexity Cr:LiCAF amplifier, which is only pumped by two 1-W tapered diodes, is capable of producing pulse energies as high as 98 μJ (~78 μJ, ~50-fs pulses with corresponding peak powers of ~1.4 GW, at up to ~5 kHz

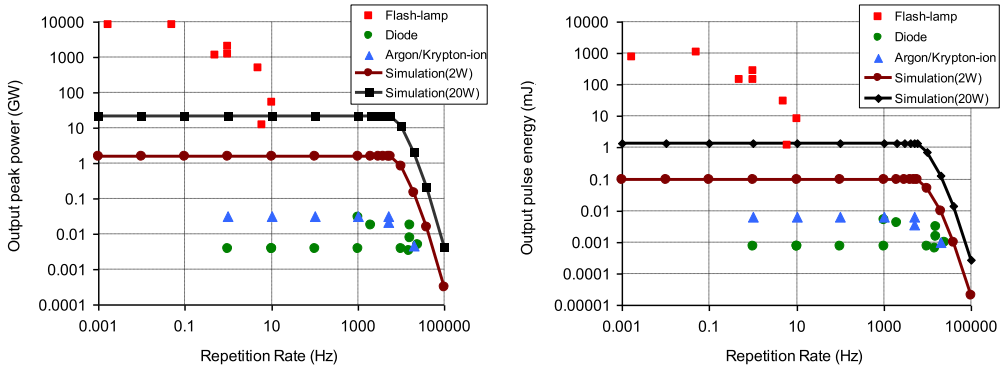

Fig. 12. Output peak powers and output pulse energies obtained from Cr:Colquiriite amplifiers to date using different pump sources. Simulation results for the 2-W and 20-W pumped Cr:LiCAF amplifier is also included for comparison.

after compression). The results can further be improved using more complex pumping schemes, and as an example, a 20-W pumped Cr:LiCAF regenerative amplifier has the potential to produce pulse energies of 1.35 mJ (~1.1 mJ, ~50-fs pulses with corresponding peak powers of 20 GW, at up to ~5 kHz after compression). Moreover, expected optical-to-optical and electrical-to-optical conversion efficiencies of the amplifier systems are above 30% and 10%, respectively. The simulation results have shown that, future generation of diode pumped Cr:Colquiriite amplifiers will have the potential to improve the peak powers of regenerative amplifiers by two-to-three orders of magnitude over previous results. Compared with current state-of-the-art Ti:Sapphire ultrafast laser amplifiers, Cr:Colquiriite based amplifiers can achieve a dramatic cost savings and can have much higher electrical-to-optical and optical-to-optical conversion efficiencies.

Acknowledgments

We acknowledge partial support from TUBITAK (The Scientific and Technical Research Council of Turkey, 112T220), European Union Marie Curie Career Integration Grant (PCIG11-GA-2012–321787), and Alexander von Humboldt-Foundation.

References

[1] R.R. Gattass, E. Mazur, Nature Photonics 2 (2008) 219.
[2] S. Woutersen, U. Emmerichs, H.J. Bakker, Science 278 (1997) 658.
[3] G. Steinmeyer, D.H. Sutter, L. Gallmann, N. Matuschek, U. Keller, Science 286 (1999) 1507.
[4] G. Cerullo, M. Nisoli, S. Stagira, S. De Silvestri, Optics Letters 23 (1998) 1283.
[5] D. Brida, S. Bonora, C. Manzoni, M. Marangoni, P. Villoresi, S. De Silvestri, G. Cerullo, Optics Express 17 (2009) 12510.
[6] D. Brida, G. Cirmi, C. Manzoni, S. Bonora, P. Villoresi, S. De Silvestri, G. Cerullo, Optics Letters 33 (2008) 741.
[7] P.M. Paul, E.S. Toma, P. Breger, G. Mullot, F. Auge, P. Balcou, H.G. Muller, P. Agostini, Science 292 (2001) 1689.
[8] J. Klein, J.D. Kafka, Nature Photonics 4 (2010) 289.
[9] P.W. Roth, A.J. Maclean, D. Burns, A.J. Kemp, Optics Letters 36 (2011) 304.
[10] P.W. Roth, A.J. Maclean, D. Burns, A.J. Kemp, Optics Letters 34 (2009) 3334.
[11] C.G. Durfee, T. Storz, J. Garlick, S. Hill, J.A. Squier, M. Kirchner, G. Taft, K. Shea, H. Kapteyn, M. Murnane, S. Backus, Optics Express 20 (2012) 13677.
[12] P.W. Roth, D. Burns, A.J. Kemp, Optics Express 20 (2012) 20629.
[13] C. Horvath, A. Braun, H. Liu, T. Juhasz, G. Mourou, Optics Letters 22 (1997) 1790.
[14] C. Honninger, R. Paschotta, M. Graf, F. Morier-Genoud, G. Zhang, M. Moser, S. Biswal, J. Nees, A. Braun, G.A. Mourou, I. Johannsen, A. Giesen, W. Seeber, U. Keller, Applied Physics B-Lasers and Optics 69 (1999) 3.
[15] B.N. Samson, P.A. Tick, N.F. Borrelli, Optics Letters 26 (2001) 145.
[16] M. Larionov, F. Butze, D. Nickel, A. Giesen, Optics Letters 32 (2007) 494.
[17] R. Paschotta, Encyclopedia of Laser Physics and Technology, Wiley-VCH, 2008 〈http://eu.wiley.com/WileyCDA/WileyTitle/productCd-3527408282,descCd-description.html〉.
[18] H. Kalaycioglu, Y.B. Eldeniz, O. Akcaalan, S. Yavas, K. Gurel, M. Efe, F.O. Ilday, Optics Letters 37 (2012) 2586.
[19] J. Limpert, F. Roser, T. Schreiber, A. Tunnermann, IEEE Journal of Selected Topics in Quantum Electronics 12 (2006) 233.
[20] S.A. Payne, L.L. Chase, L.K. Smith, W.L. Kway, H.W. Newkirk, Journal of Applied Physics 66 (1989) 1051.
[21] S.A. Payne, L.L. Chase, H.W. Newkirk, L.K. Smith, W.F. Krupke, IEEE Journal of Quantum Electronics 24 (1988) 2243.
[22] L.K. Smith, S.A. Payne, W.L. Kway, L.L. Chase, B.H.T. Chai, IEEE Journal of Quantum Electronics 28 (1992) 2612.
[23] B.H.T. Chai, J.-L. Lefaucheur, M. Stalder, M. Bass, Optics Letters 17 (1992) 1584.
[24] L.K. Smith, S.A. Payne, W.F. Krupke, L.D. DeLoach, R. Morris, E.W. O'Dell, D.J. Nelson, Optics Letters 18 (1993) 200.
[25] J.F. Pinto, L. Esterowitz, G.H. Rosenblatt, IEEE Journal of Selected Topics in Quantum Electronics 1 (1995) 58.
[26] U. Demirbas, D. Li, J.R. Birge, A. Sennaroglu, G.S. Petrich, L.A. Kolodziejski, F.X. Kartner, J.G. Fujimoto, Optics Express 17 (2009) 14374.
[27] I.T. Sorokina, E. Sorokin, E. Wintner, A. Cassanho, H.P. Jenssen, R. Szipocs, Optics Letters 22 (1997) 1716.
[28] S. Uemura, K. Torizuka, Japanese Journal of Applied Physics Part 1—Regular Papers Short Notes and Review Papers 39 (2000) 3472.
[29] P. Wagenblast, U. Morgner, F. Grawert, V. Scheuer, G. Angelow, M.J. Lederer, F.X. Kärtner, Optics Letters 27 (2002) 1726.
[30] P. Wagenblast, R. Ell, U. Morgner, F. Grawert, F.X. Kärtner, Optics Letters 28 (2003) 1713.
[31] P. Beaud, M.C. Richardson, Y.F. Chen, B.H.T. Chai, IEEE Journal of Quantum Electronics 30 (1994) 1259.
[32] D. Kopf, K.J. Weingarten, G. Zhang, M. Moser, M.A. Emanuel, R.J. Beach, J.A. Skidmore, U. Keller, Applied Physics B—Lasers and Optics 65 (1997) 235.
[33] M. Stalder, M. Bass, B.H.T. Chai, Journal of Optical Society of America B 9 (1992) 2271.
[34] J.M. Eichenholz, M. Richardson, IEEE Journal of Quantum Electronics 34 (1998) 910.
[35] J.K. Jabczynski, W. Zendzian, Z. Mierczyk, Z. Frukacz, Applied Optics 40 (2001) 6638.
[36] A. Isemann, H. Hundertmark, C. Fallnich, Applied Physics B—Lasers and Optics 74 (2002) 299.
[37] A. Isemann, P. Wessels, C. Fallnich, Optics Communications 260 (2006) 211.
[38] R. Scheps, J.F. Myers, H.B. Serreze, A. Rosenberg, R.C. Morris, M. Long, Optics Letters 16 (1991) 820.
[39] P.M.W. French, R. Mellish, J.R. Taylor, P.J. Delfyett, L.T. Florez, Optics Letters 18 (1993) 1934.
[40] A. Isemann, C. Fallnich, Optics Express 11 (2003) 259.
[41] D. Li, U. Demirbas, J.R. Birge, G.S. Petrich, L.A. Kolodziejski, A. Sennaroglu, F.X. Kartner, J.G. Fujimoto, Optics Letters 35 (2010) 1446.
[42] B. Sumpf, K.H. Hasler, P. Adamiec, F. Bugge, F. Dittmar, J. Fricke, H. Wenzel, M. Zorn, G. Erbert, G. Trankle, IEEE Journal of Selected Topics in Quantum Electronics 15 (2009) 1009.
[43] B. Sumpf, P. Adamiec, M. Zorn, H. Wenzel, G. Erbert, IEEE Photonics Technology Letters 22 (2011) 266.
[44] U. Demirbas, M. Schmalz, B. Sumpf, G. Erbert, G.S. Petrich, L.A. Kolodziejski, J.G. Fujimoto, F.X. Kärtner, A. Leitenstorfer, Optics Express 19 (2011) 20444.
[45] M.D. Perry, D. Strickland, T. Ditmire, F.G. Patterson, Optics Letters 17 (1992) 604.
[46] W.E. White, J.R. Hunter, L. Vanwoerkom, T. Ditmire, M.D. Perry, Optics Letters 17 (1992) 1067.
[47] P. Beaud, E. Miesak, Y.F. Chen, B.H.T. Chai, M.C. Richardson, Optics Communications 95 (1993) 46.
[48] P. Beaud, M. Richardson, E.J. Miesak, B.H.T. Chai, Optics Letters 18 (1993) 1550.
[49] T. Ditmire, H. Nguyen, M.D. Perry, Journal of the Optical Society of America B—Optical Physics 11 (1994) 580.
[50] T. Ditmire, H. Nguyen, M.D. Perry, Optics Letters 20 (1995) 1142.
[51] T. Ditmire, M.D. Perry, Optics Letters 18 (1993) 426.
[52] T. Ditmire, M.D. Perry, Generation, Amplification, and Measurement of Ultrashort Laser Pulses II 2377 (1995) 301.
[53] R.E. Samad, G.E.C. Nogueira, S.L. Baldochi, N.D. Vieira, Solid State Lasers Xvi: Technology and Devices 6451 (2007) 45112.
[54] R.E. Samad, G.E.C. Nogueira, S.L. Baldochi, N.D. Vieira, Journal of Optics A—Pure and Applied Optics 10 (2008).
[55] R.E. Samad, G.E.C. Nogueira, S.L. Baldochi, N.D. Vieira, Riao/Optilas 992 (2008) 398. (1343).
[56] F. Balembois, P. Georges, F. Salin, A. Brun, Optics Letters 18 (1993) 1250.
[57] S.C.W. Hyde, N.P. Barry, R. Mellish, P.M.W. French, J.R. Taylor, C.J.v.d. Poel, A. Valster, Optics Letters 20 (1995) 160.
[58] F. Balembois, P. Georges, A. Brun, Mode-Locked and Solid State Lasers, Amplifiers, and Applications 2041 (1994) 88. (446).
[59] N.P. Barry, S.C.W. Hyde, R. Mellish, P.M.W. French, J.R. Taylor, C.J. Vanderpoel, A. Valster, Electronics Letters 30 (1994) 1761.
[60] R. Mellish, N.P. Barry, S.C.W. Hyde, R. Jones, P.M.W. French, J.R. Taylor, C.J.v.d. Poel, A. Valster, Optics Lett 20 (1995) 2312.
[61] E. Sorokin, in: F.X. Kärtner (Ed.), Few-cycle Laser Pulse Generation and its Applications, 95, Springer-Verlag, Berlin, 2004, p. 3.
[62] L.G. DeShazer, K.W. Kangas, Conference on Lasers and Electro Optics 14 (1987) 296.
[63] U. Demirbas, S. Eggert, A. Leitenstorfer, Journal of Optical Society of America B 29 (2012) 1894.
[64] I.T. Sorokina, E. Sorokin, E. Wintner, A. Cassanho, H.P. Jenssen, M.A. Noginov, Optics Letters 21 (1996) 204.
[65] U. Demirbas, R. Uecker, D. Klimm, J. Wang, Applied Optics 51 (2012) 8440.
[66] R. Ell, U. Morgner, F.X. Kärtner, J.G. Fujimoto, E.P. Ippen, V. Scheuer, G. Angelow, T. Tschudi, Optics Letters 26 (2001) 373.
[67] F. Druon, F. Balembois, P. Georges, Comptes Rendus Physique 8 (2007) 153.
[68] A. Sanchez, R.E. Fahey, A.J. Strauss, R.L. Aggarwal, Optics Letters 11 (1986) 363.
[69] P.F. Moulton, JOSA B 3 (1986) 125.
[70] L.J. Atherton, S.A. Payne, C.D. Brandle, Annual Review of Materials Science 23 (1993) 453.
[71] D. Klimm, G. Lacayo, P. Reiche, Journal of Crystal Growth 210 (2000) 683.
[72] V.V. Fedorov, S.B. Mirov, A. Gallian, D.V. Badikov, M.P. Frolov, Y.V. Korostelin, V.I. Kozlovsky, A.I. Landman, Y.P. Podmar'kov, V.A. Akimov, A.A. Voronov, IEE Journal of Quantum Electronics 42 (2006) 907.
[73] M. Stalder, M. Bass, B.H.T. Chai, Journal of Optical Society of America B 9 (1992) 2271.
[74] D. Kopf, U. Keller, M.A. Emanuel, R.J. Beach, J.A. Skidmore, Optics Letters 22 (1997) 99.
[75] D. Kopf, J.A. Derau, U. Keller, G.L. Bona, Optics Letters 20 (1995) 1782.
[76] S.A. Payne, L.L. Chase, L.J. Atherton, J.A. Caird, W.L. Kway, M.D. Shinn, R.S. Hughes, L.K. Smith, SPIE Solid State Lasers (1990) 84.
[77] H.W.H. Lee, S.A. Payne, L.L. Chase, Physical Review B 39 (1989) 8907.
[78] P. Beaud, Y.-F. Chen, B.H.T. Chai, M.C. Richardson, Optics Letters 17 (1992) 1064.

[79] P.A. Beaud, M. Richardson, E.J. Miesak, IEEE Journal of Quantum Electronics 31 (1995) 317.
[80] V. Pilla, H.P. Jenssen, A. Cassanho, T. Catunda, Optics Communications 271 (2007) 184.
[81] Z.L. Liu, T. Kozeki, Y. Suzuki, N. Sarukura, K. Shimamura, T. Fukuda, M. Hirano, H. Hosono, Optics Letters 26 (2001) 301.
[82] L.M. Frantz, J.S. Nodvik, Journal of Applied Physics 34 (1963) 2346.
[83] C. Rouyer, E. Mazataud, I. Allais, A. Pierre, S. Seznec, C. Sauteret, G. Mourou, A. Migus, Optics Letters 18 (1993) 214.
[84] U. Demirbas, A. Sennaroglu, F.X. Kärtner, J.G. Fujimoto, Optics Letters 34 (2009) 497.
[85] U. Demirbas, K.H. Hong, J.G. Fujimoto, A. Sennaroglu, F.X. Kartner, Optics Letters 35 (2010) 607.